ISSN 1330-3651 (Print), ISSN 1848-6339 (Online) https://doi.org/10.17559/TV-20200804125931
Original scientific paper

Single-Loop Full R Joints of Multi-Mode Omnidirectional Ground Mobile Robot

Chunyan ZHANG*, Xinxing JIANG, Xiangyu LIU, Dan ZHANG

Abstract: In order to solve the problem of loss of locomotion ability due to overturning and instability during the movement of a mobile robot, a multi-mode omnidirectional ground mobile robot with a deformable structure is proposed. Single-loop is used as the unit, and the three-direction geometric deformation can be realized by controlling its R joints in time sharing. The 4-RRRRRR parallel mobile robot formed by two closed-loops orthogonally has four different rolling modes, and each mode can be switched between each other. Once the robot is overturned and unstable during the movement, it can be deformed into other modes and continue to move. After the description of the robot, the DOF (degree-of-freedom) is calculated based on the screw theory. Gait planning and locomotion feasibility analysis indicate that the robot can realize four locomotion modes and their mutual switching. Finally, the simulations and prototype experiments are presented to verify the feasibility of the different locomotion modes and the ability of the obstacle crossing.

Keywords: Multi-mode; Obstacle crossing; Omnidirectional mobile robot; Single-loop

1 INTRODUCTION

Omnidirectional mobile robots mainly include wheel-leg hybrid robots, wheel-track hybrid robots and wheel-leg-track hybrid robots [1-8]. These kinds of robots have the ability of rapid locomotion of wheeled robot and obstacle surmounting of leg robot and crawler robot. Compared with wheeled, legged and tracked robots in a single locomotion mode, its excellent mobile performance and obstacle surmounting ability make it more adaptable to complex terrain, so that it can better apply military reconnaissance, space exploration, anti-terrorist explosive disposal and other unstructured and complicated operational tasks. Therefore, the research on omnidirectional mobile robots is of great significance and attracts more and more scholars' attention.

Many scholars and research institutions have proposed a variety of omnidirectional mobile robots. Wang et al [9] proposed a new type of linkage articulated wheel-leg mobile robot with three motion modes, which can adapt to complex terrain environments; Luo [10] proposed a novel reconfigurable hybrid wheel-tracked mobile robot which has three locomotion modes; Jiang et al [11] proposed a wheel-leg mobile robot that can actively adjust its posture according to the terrain environment and can traverse unstructured terrain environments; Jesus.M et al [12] proposed a wheel-legged hybrid robot, which can climb continuous steps and has a strong obstacle-crossing capability. Although the omnidirectional mobile robots that have been developed so far have a variety of mobile capabilities, they have problems such as complex structure, cumbersome control, and large volume.

In order to solve these problems, Yao et al [13-16] systematically explored the configuration design method, movement mode analysis and movement capability analysis of the link mechanism, taking the deformation movement of the link mechanism as the main research direction, and proposed a series of planar and spatial links robot model. Wang et al [17] designed a rolling robot that can switch modes between planar linkage mode and spherical linkage mode by floding and spreading; Tian et al used single loop linkages to realize different locomotion modes by changing their gestures, they presented a mobile parallelogram mechanism that can slide or crawl on the ground [18], and used a spatial 8R linkage to realize biped and rolling locomotion [19]. Taking the plane 6R linkage as the unit, He et al [20] proposed a mobile robot that can adapt to a variety of complex terrain environments; Liu CH [21] proposed an 8U parallel mechanism with omnidirectional rolling capability; Wang et al [22] proposed a mobile robot that uses self-reconfiguration to achieve multiple motion modes; Zhang et al [23] proposed a multi-mode mobile robot with self-traversal based on parallel mechanism; Phipps et al [24] proposed a kind of rolling robot which can switch locomotion modes between a circle or spherical robot and a legged robot; Li et al [25] proposed a 4-RSR parallel rolling robot that can switch between multiple mobile modes.

However, once such robots fall over or lose their stability in the process of movement, they are likely to lose their ability to move and cannot complete the task. Therefore, the research on how to overcome the problem of losing locomotion ability due to overturning and instability in the process of locomotion is an important problem to be considered in the design and analysis of this kind of robots. This paper presents a reconfigurable multi-mode omnidirectional mobile robot. The robot not only has four kinds of locomotion modes that can be flexibly switched between different modes to adapt to various terrains but also has the ability to make the robot continue to move through the geometric deformation of the mechanism in the case of overturning and instability.

2 MECHANISM DESIGN AND DOF ANALYSIS

2.1 Mechanism Design

The robot consists of the upper platform $(A_1 - A_4)$, the lower platform $(F_1 - F_4)$ and four limbs with the same structure, which are symmetrically distributed (Fig. 1). The sketch of the mechanism is shown in Fig. 2.

Among them, each limb consists of six R joints $R_{i1} \sim R_{i6}$ $(i = 1 \sim 4)$ at A_i, B_i, C_i, D_i, E_i and F_i. Each limb is respectively connected with the upper and lower platforms through the R joints $R_{i1}R_{i6}$ of the common axis. The limb 1(2), limb 3(4), and the upper and lower platforms form two spatially orthogonal full R closed-loops, which are also a 4-RRRRRR parallel mechanism.

As shown in Fig. 2, its initial state, a coordinate system $O-XYZ$ is attached to the center of platform F_i, X - axis and Y - axis are along the two axes of the joints R_{25}, R_{45} and R_{15}, R_{35} respectively, and Z - axis can be obtained by the right-hand rule.

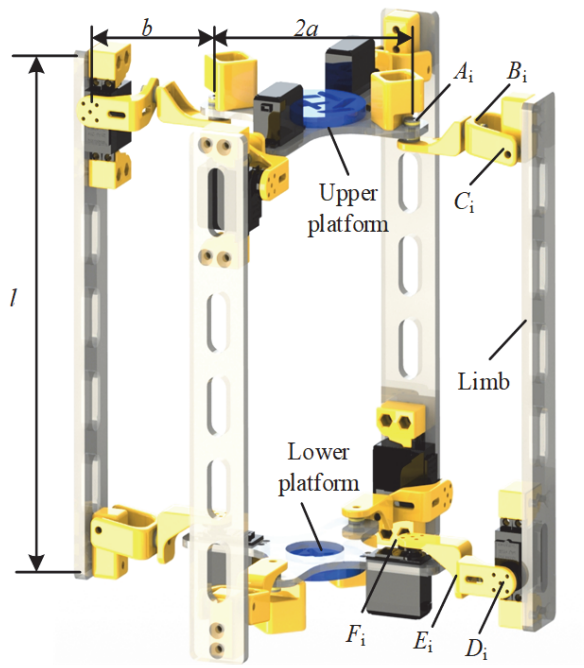

Figure 1 3D model of the robot

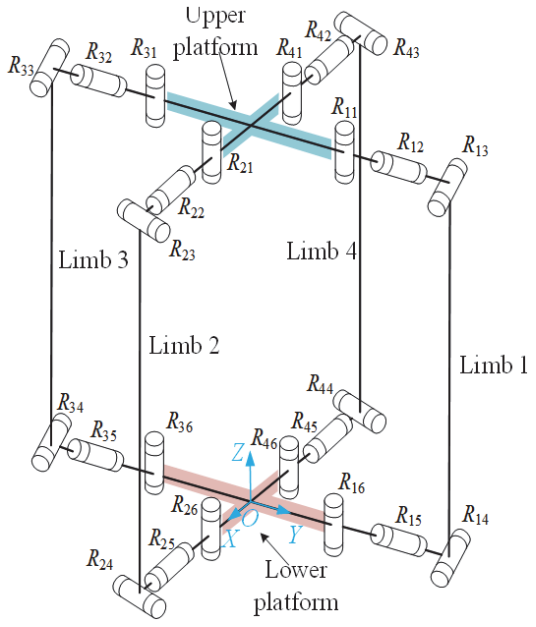

Figure 2 Sketch of robot mechanism

A single-loop full R joints composed of limbs 1, 3 and upper and lower platforms are shown in Fig. 3. It consists of 12 R joints. The axes of the rotating pair $R_{13}, R_{33}, R_{14}, R_{34}$ are parallel to the X - axis. The axes of the rotating pair $R_{12}, R_{32}, R_{15}, R_{35}$ are parallel to the Y - axis. The axes of the rotating pair $R_{11}, R_{31}, R_{16}, R_{36}$ are parallel to the Z - axis. Each group of R joints can form a plane $4R$ mechanism. The Single-loop can realize the rotation around the X - axis, Y - axis and Z - axis respectively so that the mobile robot can realize variable width rotation in X and Y directions, omnidirectional rolling around X and Y directions, side rolling around Z direction and spherical rolling as shown in Tab. 1.

The dimension relations of links on each limb are as follows: $\|A_1A_3\| = \|F_1F_3\| = 2a$, $\|A_iC_i\| = \|D_iF_i\| = b$, $(i=1,3)\|C_iD_i\| = l(i=1,3)$. Let θ_1, θ_3 be the rotation angle of limb 1 and 3 around axis $R_{11}R_{16}, R_{31}R_{36}$ respectively. Make it turn counterclockwise at a positive angle. Let θ_5, θ_7 be the rotation angle of closed-loop around R_{14}, R_{34} . which are parallel to X - axis. The same is true of the single-loop $C_2C_4D_4D_2$. Let θ_2, θ_4 be the rotation angle of limb 2 and 4 around axes $R_{21}R_{26}, R_{41}R_{46}$ respectively. Let θ_6, θ_8 be the rotation angle of closed-loop around R_{24}, R_{44} which are parallel to X - axis. The first locomotion mode of the robot is defined as the initial configuration.

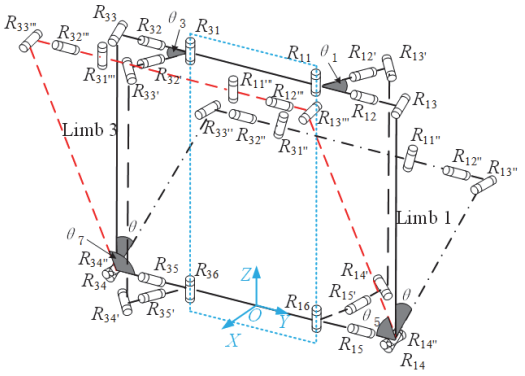

Figure 3 Single-loop full R joints structure diagram

Table 1 Multi-mode omnidirectional mobile robot with four locomotion modes

Omnidirectional rolling	variable width rolling
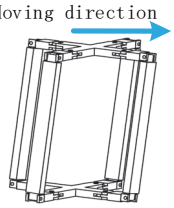	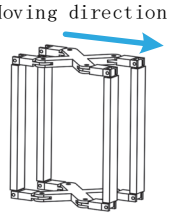
side rolling	spherical rolling
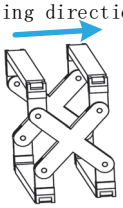	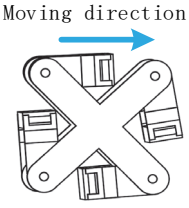

2.2 DOF Analysis

In order to analyze the DOF of mobile robot in four different locomotion modes, a coordinate system $o-x_1y_1z_1$ is set up on the limb 1. Its origin point o is at the center of F_1 joint, x_1 - axis is parallel to X - axis, y_1 - axis is parallel to Y - axis. According to the screw theory [26], the DOF of the mobile robot can be established as shown in Tab. 2.

Table 2 DOF analysis

mode	limb	Twist system	Wrench system
Omnidirectional rolling	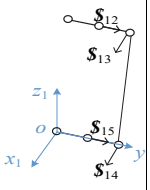	$\$_{12}=(0\,1\,0;a_2\ 0\ c_2)$ $\$_{13}=(1\,0\,0;0\ b_3\ c_3)$ $\$_{14}=(1\,0\,0;0\ 0\ c_4)$ $\$_{15}=(0\,1\,0;0\ 0\ c_5)$	$\$^r_{11}=(0\,0\,0;0\,0\,1)$ $\$^r_{12}=(a_6\ 0\,1;b_6\ c_6\ 0)$
variable width rolling	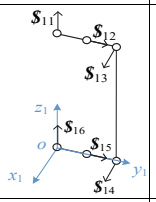	$\$_{11}=(0\ 0\ 1;a_1\ 0\ 0)$ $\$_{12}=(0\ 1\ 0;a_2\ 0\ c_2)$ $\$_{13}=(1\ 0\ 0;0\ b_3\ c_3)$ $\$_{14}=(1\ 0\ 0;0\ 0\ c_4)$ $\$_{15}=(0\ 1\ 0;0\ 0\ c_5)$ $\$_{16}=(0\ 0\ 1;0\ 0\ 0)$	none
Side/spherical rolling	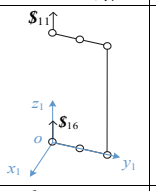	$\$_{11}=(0\ 0\ 1;0\ 0\ 0)$ $\$_{16}=(0\ 0\ 1;0\ 0\ 0)$	$\$^r_{11}=(1\,0\,0;0\,0\,0)$ $\$^r_{12}=(0\,1\,0;0\,0\,0)$ $\$^r_{13}=(0\,0\,1;0\,0\,0)$ $\$^r_{14}=(0\,0\,0;1\,0\,0)$ $\$^r_{15}=(0\,0\,0;0\,1\,0)$
	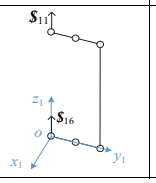	$\$_{11}=(0\ 0\ 1;0\ 0\ 0)$ $\$_{16}=(0\ 0\ 1;0\ 0\ 0)$	$\$^r_{11}=(1\,0\,0;0\,0\,0)$ $\$^r_{12}=(0\,1\,0;0\,0\,0)$ $\$^r_{13}=(0\,0\,1;0\,0\,0)$ $\$^r_{14}=(0\,0\,0;1\,0\,0)$ $\$^r_{15}=(0\,0\,0;0\,1\,0)$

As can be seen from Tab. 2, when the robot is in the omnidirectional rolling mode, the DOF is calculated as 2, which is the rotational around the X and Y - axes respectively. When the robot is in the variable width rolling mode, the DOF is calculated as 6, which are: the four limbs rotate around the Z - axis and the rotational around the X - axis and Y - axis respectively. When the robot is in the mode of side rolling and spherical rolling, the DOF is calculated as 4, which are the four limbs rotating around the Z - axis respectively.

3 ANALYSIS OF GAIT PLANNING IN DIFFERENT LOCOMOTION MODES

A reasonable gait planning can make the robot realize various locomotion modes and their mutual switching.

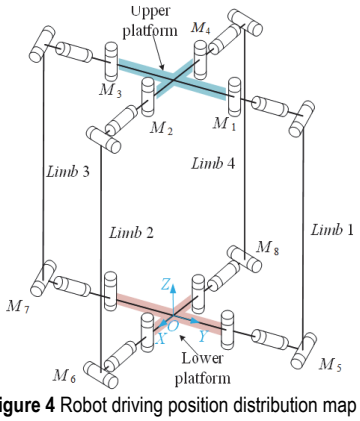

Figure 4 Robot driving position distribution map

By analyzing the gait of each locomotion mode, eight motors M_1-M_8 are set to control the robot in different configures as shown in Fig. 4. Among them, M_1-M_4 are assembled on R joints R_{11},R_{21},R_{31} and R_{41} respectively; M_5-M_8 are mounted on R_{14},R_{24},R_{34} and R_{44} respectively.

3.1 Analysis of Gait Planning in Omnidirectional Rolling Mode

When the axes of joints R_{11} and R_{16}, R_{21} and R_{26}, R_{31} and R_{36}, R_{41} and R_{46} are collinear, lock M_1-M_4, then the robot turns to the initial state of omnidirectional rolling mode (Fig. 5a). Drive motors M_5, M_8 in sequence, the robot tilt around the X - axis and Y - axis successively (Fig. 5b) and turn over, so as to reach the landing posture of two limbs (Fig. 5c). Continue to drive motors M_5, M_8, the robot rotates around C_1C_4. Under the action of inertial force, the robot tilts and overturns to reach the landing state of the upper platform (Fig. 5d). Continue to drive the motors, the robot returns to the initial state of landing on the upper platform (Fig. 5e), thus completing a cycle of rolling.

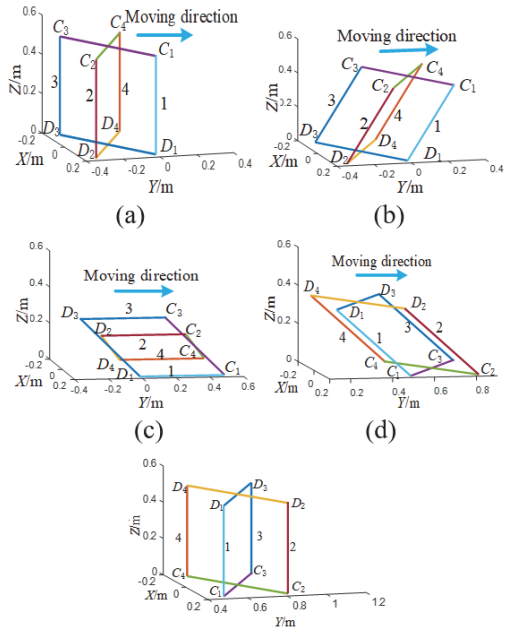

Figure 5 Omnidirectional rolling gait diagram

In the same way, driving motors M_5M_6, M_6M_7 and M_7M_8 can realize the rolling of the robots in other three directions D_1D_2, D_2D_3 and D_3D_4 respectively.

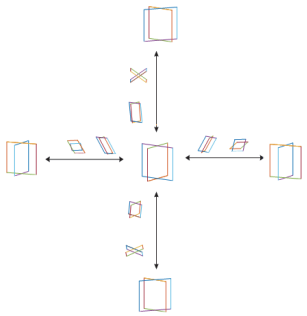

Figure 6 Omnidirectional rolling gait planning of robot

Therefore, in this mode, the robot can roll in four directions: forward, backward, left and right (Fig. 6). It can adjust back to the original state and continue to move through this ability in case of overturning and instability during the moving process.

3.2 Gait Planning in Variable Width Rolling Mode

When the axes of joints R_{11} and R_{16}, R_{21} and R_{26}, R_{31} and R_{36}, R_{41} and R_{46} are collinear, drive $M_1 - M_4$ synchronously, the four limbs rotate in the opposite direction (or vice versa) around the four collinear axes $R_{i1}R_{i6}$ $(i = 1 \sim 4)$, and change the overall width of the robot along the X - axis (or Y - axis). The motors are then sequentially driven to repeat the previous locomotion mode, thus completing a cycle of variable width rolling mode as shown in Fig. 7

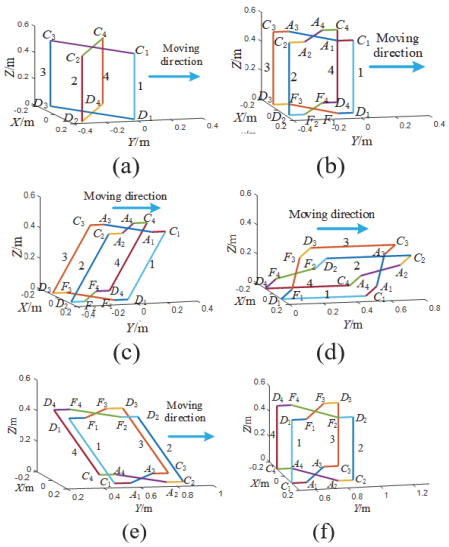

Figure 7 Variable width rolling gait diagram

3.3 Gait Planning in Side Rolling Mode

When the robot in the state of two limbs 1 and 2 is contacting with the ground at the same time (Fig. 8a), lock $M_5 - M_8$, drive motors $M_1 - M_4$, the limbs 1, 2, 3 and 4 rotate, and the robot rotates around the Z - axis to tilt to the right (Fig. 8b).

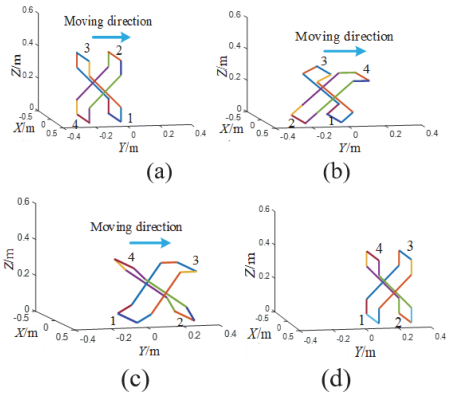

Figure 8 Roll gait diagram

Continue to drive motors $M_1 - M_4$ to make the robot topple over and reach the other two limbs 1 and 2 on the ground (Fig. 8c), thus completing a cycle of rolling (Fig. 8d). This rolling mode can be regarded as discrete points due to the landing point of the limbs. Therefore, it is possible to overcome obstacles on uneven ground, ditches and steps.

3.4 Gait Planning in Spherical Rolling Mode

Lock $M_5 - M_8$, the robot is in the initial state of the spherical rolling mode, when the robot in the state of one limb 2 connecting with the ground (Fig. 9a), driving M_2 to let robot rotate around Z - axis (Fig. 9b). The robot tilts and overturns (as shown in Fig. 9c) to reach the landing state of another limb c (as shown in Fig. 9d). Repeat the above actions in turn to complete a spherical periodic rolling.

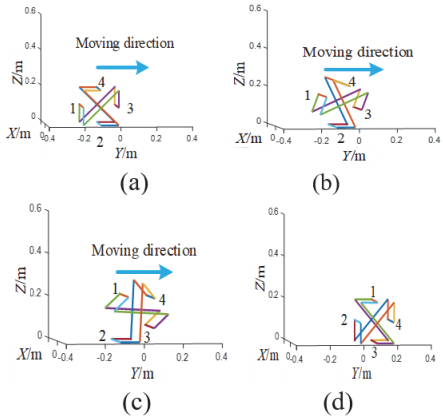

Figure 9 Sphere-like rolling gait diagram

3.5 Gait Switching Strategies for Four Locomotion Modes

According to the gait planning analysis of the above-mentioned locomotion modes, the four locomotion modes of the robot can switch to each other, and the switching strategy is shown in Fig. 10.

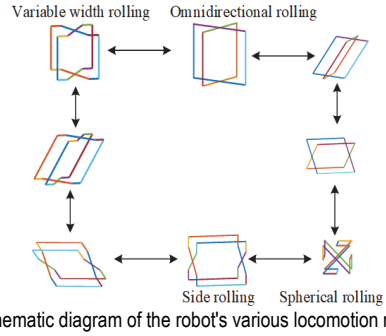

Figure 10 Schematic diagram of the robot's various locomotion mode switching strategies

According to the switching strategy, the initial state of the robot can be any state of the above four modes. When the robot is in the initial state of omnidirectional rolling mode, it is possible to switch to the variable width rolling mode by changing the width of the four limbs. It can be switched to side rolling mode via drive motors $M_5 - M_8$. Then by driving motors $M_1 - M_4$, it can be switched to the

spherical rolling mode. The robot reaches the landing state of two limbs firstly, then it can switch back to the initial state of omnidirectional rolling after dumping, thus realizing the gait switching among four locomotion modes.

Through the gait analysis of the above locomotion modes, the robot can realize four locomotion modes by time-sharing control of the motor [27].

4 FEASIBILITY ANALYSIS OF EACH LOCOMOTION MODE

4.1 Feasibility Analysis of Omnidirectional Rolling Mode

During the rolling process, the condition that the robot can keep stable is that the zero moment point (ZMP) must always be in the support area [5]. Therefore, the condition for the robot to achieve omnidirectional rolling is whether the robot is in an unstable state, that is, whether the ZMP point can fall outside the support area. In this paper, ZMP [22] is used to investigate the conditions for the robot to achieve omnidirectional rolling.

The coordinates of ZMP are expressed as:

$$x_{\text{zmp}}=\frac{\sum_{i=0}^{n}m_i(\ddot{z}_i+g_z)x_i-\sum_{i=0}^{n}m_i\ddot{x}_i z_i-\sum_{i=0}^{n}J_i\alpha_{i,y}}{\sum_{i=0}^{n}m_i(\ddot{z}_i+g_z)} \tag{1}$$

$$y_{\text{zmp}}=\frac{\sum_{i=0}^{n}m_i(\ddot{z}_i+g_z)y_i-\sum_{i=0}^{n}m_i\ddot{y}_i z_i-\sum_{i=0}^{n}J_i\alpha_{i,x}}{\sum_{i=0}^{n}m_i(\ddot{z}_i+g_z)} \tag{2}$$

where m_i is the mass of the *i*-th member, $\ddot{y}_i$ and $\ddot{z}_i$ are the acceleration of the *i*-th member in the Y - axis and Z - axis directions respectively, x_i, y_i and z_i are the *i*-th position of CM (center of mass), g_z is the gravitational acceleration, J_i is the moment of inertia of member *i*, and $\alpha_{i,x}$ and $\alpha_{i,y}$ are the angular acceleration of member *i* in the X - axis and Y - axis directions respectively.

Assuming that all members of the mechanism are of uniform mass, symmetrical shape and geometric center of mass, the simplified mechanism contains 14 members. When i = 0, member i is the lower platform. When $i=1\sim4$, member i is the link C_iD_i. When $i=5\sim12$, member i is the link A_iC_i. When $i=13$, member i is the upper platform. According to the requirements of ZMP calculation, the design parameters are determined $m_0=m_{13}=0.2$ kg , $m_i(i=1\sim4)=0.4$ kg , $m_i(5\sim12)=0.05$ kg , $a=0.14$ m, $b=0.09$ m, $l=0.5$ m .

The support area of the robot is shown in Fig. 11. The driving angles of motors M_5 , M_6 are the same, when x_{ZMP} and y_{ZMP} are beyond the critical point (0.115, 0.115) in the plane, the robot will tumble.

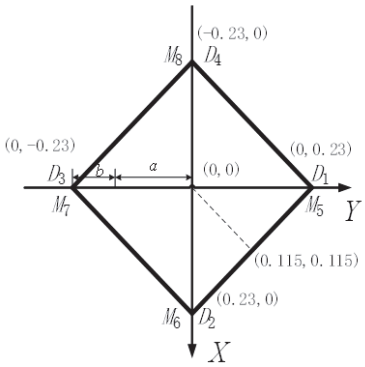

Figure 11 Robot omnidirectional rolling stable area

Due to the structural symmetry of the mechanism, the variation trends of x_{ZMP} and y_{ZMP} are the same. As shown in Fig. 12, *data*1 , *data*2 and *data*3 represent the corresponding curve of the mechanism at velocity $\dot{\theta}_5=\dot{\theta}_6=\pi, 0, 2\pi$ rad/s respectively. When $\dot{\theta}_5=\dot{\theta}_6=\pi 2\pi$ rad/s , if the rotation angle of the drive angle is greater than 57.3° or 51.7°, respectively, the ZMP curves have parts that are beyond the line $x_{\text{ZMP}}=y_{\text{ZMP}}=0.115$, so the rolling of the mechanism in this mode is feasible.

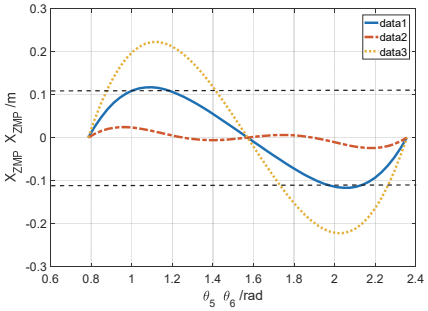

Figure 12 x_{ZMP} y_{ZMP} curve

4.2 Feasibility Analysis of Variable Width Rolling Mode

When the robot is in variable width rolling mode, as the omnidirectional rolling mode has been analyzed previously, that is $\theta_1=\theta_2=\theta_3=\theta_4=0^\circ$, it is only necessary to select the limit position, which is $\theta_1=\theta_3=45^\circ$, $\theta_2=\theta_4=-45^\circ$ for locomotion feasibility analysis.

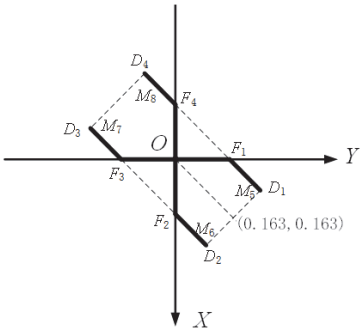

Figure 13 Robot variable width rolling stable area

If the robot can roll at this limit position, the robot can roll in the whole process of variable width. Analyze the

stability of robot using ZMP principle. If the x_{ZMP}, y_{ZMP} of the robot can exceed the support area shown in Fig. 13, then the mechanism will tumble.

The Eq. (1) and Eq. (2) are used to calculate the ZMP of the mechanism. Due to the symmetry of the mechanism, the input angles $\theta_5 = \theta_6$, x_{ZMP} and y_{ZMP} in this mode are consistent.

As shown in Fig. 15, when the lower platform is the support surface, the support area of the mechanism is a rectangle $D_1D_2D_3D_4$ enclosed by the lower platform and links $D_iF_i(i=1\sim4)$. When x_{ZMP} and y_{ZMP} go beyond the point (0.163, 0.163) in the plane, the robot will tumble. When the input angular velocity $\dot{\theta}_5 = \dot{\theta}_6 = \frac{\pi}{4}, \frac{\pi}{2}, \frac{3\pi}{4}$ rad/s, the ZMP curve along the X - axis and Y - axis is shown in Fig. 14. Among them, *data*1, *data*2 and *data*3 are the corresponding curves of $\dot{\theta}_5 = \dot{\theta}_6 = \frac{\pi}{4}, \frac{\pi}{2}, \frac{3\pi}{4}$ rad/s respectively. It can be seen from the diagram that at $\dot{\theta}_5 = \dot{\theta}_6 = \frac{\pi}{2}, \frac{3\pi}{4}$ rad/s, if the rotation angle of the drive angle is greater than 45.8°, the ZMP curves have parts beyond the line $x_{ZMP} = y_{ZMP} = 0.163$. Therefore, the robot will tumble.

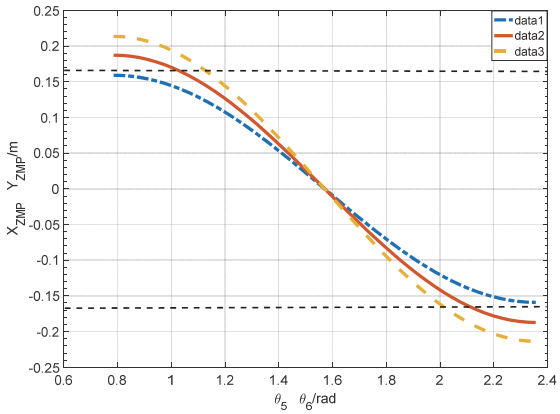

Figure 14 x_{ZMP} y_{ZMP} curve

4.3 Feasibility Analysis of Side Rolling Mode

Since the robot roll gait planning is based on the static process [13], the key point to complete the roll gait is whether the CM of the robot is beyond the support area. As shown in Fig. 15, when the mechanism is in a roll mode, it can be simplified as a flat five-bar mechanism.

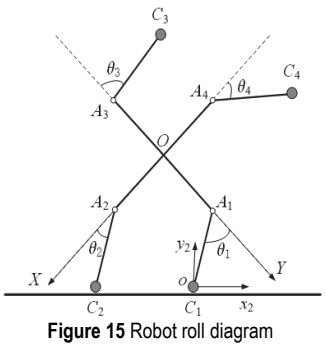

Figure 15 Robot roll diagram

The central crossbar represents the two platforms, and the four links $A_1C_1, A_2C_2, A_3C_3, A_4C_4$ connected to it represent the corresponding limbs 1, 2, 3, 4 respectively.

According to the structural characteristics of the mechanism and the position of motors, it is set that the mass at A_i is M_A and at C_i is M_C. In the coordinate system $O-XY$, the CM of the mechanism can be expressed as:

$$\boldsymbol{r}_{CM} = \frac{bm_C}{4(m_A+m_C)}\begin{bmatrix}\sin\theta_1+\cos\theta_2\\-\sin\theta_3-\cos\theta_4\\\cos\theta_1-\sin\theta_2\\-\cos\theta_3+\sin\theta_4\end{bmatrix} \tag{3}$$

Further using $C_i(i=1)$ as the origin of coordinates, the global coordinate system $o-x_2y_2$ is established. Suppose that A_3C_3, A_4C_4 remain parallel at the beginning, that is $|\theta_1|+|\theta_2|=90^\circ$. In this case, the transformation relationship between the coordinate system $O-XY$ and the coordinate system $o-x_2y_2$ can be obtained as:

$${}^{o}\boldsymbol{T}_O = \begin{bmatrix}-k_3 & k_3 & k_1-ak_3\\-k_3 & -k_3 & ak_3+k_2\\0 & 0 & 1\end{bmatrix} \tag{4}$$

Among them, $k_1 = b\cos(\theta_1+45^\circ), k_2 = b\sin(\theta_1+45^\circ)$, $k_3 = \sqrt{2}/2$.

It can be concluded that the homogeneous matrix of the CM in the coordinate system $o-x_2y_2$ can be expressed as:

$${}^{o'}\boldsymbol{R}_{CM} = {}^{o'}\boldsymbol{T}_O\begin{bmatrix}\boldsymbol{r}_{CM}\\1\end{bmatrix} = \begin{bmatrix}-k_3r_{CM,x}+k_3r_{CM,y}+k_1-ak_3\\-k_3r_{CM,x}-k_3r_{CM,y}+k_1+ak_3\\1\end{bmatrix} \tag{5}$$

It can be seen from Fig. 19 that the condition for the mechanism to roll is $R_{CM,x} > 0$.

According to the structural parameters of the mechanism, it can be obtained that θ_1 is 77.35°.

4.4 Feasibility Analysis of Spherical Rolling

When the robot is in the spherical rolling mode, it can be simplified as a five-bar mechanism as shown in Fig. 16. The plane coordinate system $o-x_3y_3$ with point A_1 as its origin is established.

According to the structural parameters of the mechanism, the CM in the X - axis direction can be obtained when the mechanism is in this state.

$$X_G = \left(0.196\cos\theta - 0.099\cos(\theta+\pi/4) - \right.\\ \left. -0.0495\cos(\theta-\pi/4)+0.0495\right) \Big/ 2.4 \tag{6}$$

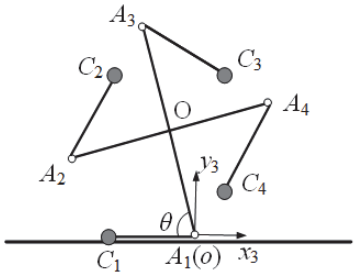

Figure 16 Sphere scrolling diagram

Among them, $\theta = \pi - \theta_1$, take $\theta \in (0.2\pi/3)$. Fig. 17 shows the relationship between the robot's CM coordinates and the rotation angle θ. As can be seen from Fig. 17, when the rotation angle θ goes beyond 93.63° (1.634 rad), the robot will turn over and realize the rolling locomotion.

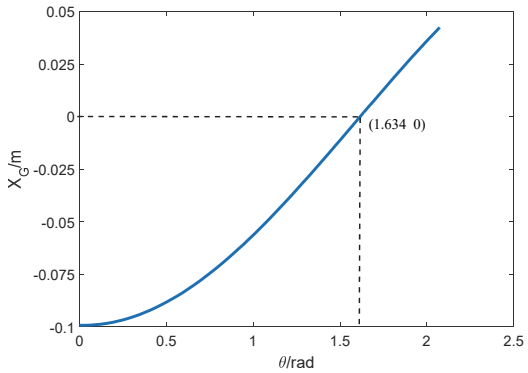

Figure 17 The relationship between the center of mass coordinates and the rotation angle of the robot

5 SIMULATION OF VARIOUS LOCOMOTION MODES AND ANALYSIS OF OBSTACLE SURMOUNTING PERFORMANCE

In order to verify the rationality of the robot scheme design and the feasibility of locomotion planning, the simulation with Adams is carried out. According to the structural characteristics of different locomotion modes of the robot, the obstacle crossing performance of the robot is also analyzed.

5.1 3D Model Import Aand Add Driver

Import the 3D model into the ADAMS software and set its parameters. Adopt STEP function to control the corresponding drive, its form is: when the driving joint needs to be locked, the function is STEP (time, 0, 0, 1, 0). It indicates that the joint is locked within 0 to 1 second. When the driving joint needs to rotate by a certain angle, the function is STEP (time, 0, 0, 1, 45 d). It means that the joint rotates 45° in 0 to 1 second. The static friction coefficient between the robot and the ground is 0.3, the dynamic friction coefficient is 0.1, the static friction transformation speed is 100.0 mm/sec, and the friction transformation speed is 1000 mm/s. The model after adding the rotating pair and driving is shown in Fig. 18.

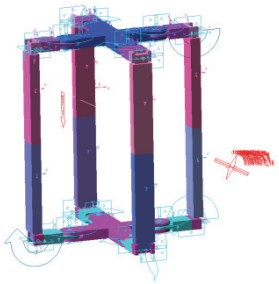

Figure 18 Model diagram after adding motion pair and drive

5.2 Simulation Analysis of Omnidirectional Rolling Mode

The robot is in the landing state of the lower platform, and first drives the motors M_5, M_8 at an angular velocity of $\omega = \pi$ rad/s. When the driving angle is more than 47°, the robot realizes the first step of overturning. At this time, the two branches are on the ground. Continue to drive the motors M_5, M_8 at an angular speed of $\omega = 2\pi$ rad/s. Under the action of inertial force, when the driving angle is more than 58°, the robot realizes the second step of overturning. At this time, the robot reaches the state where the upper platform touches the ground to realize the omnidirectional rolling motion of the robot. As shown in Fig. 19 is one-cycle of omnidirectional rolling mode.

Figure19 Omnidirectional scroll mode

5.3 Locomotion Simulation and Obstacle Crossing Analysis of Variable Width Rolling Mode

In this mode, the robot can change the overall width of the mechanism by controlling the corresponding motors, which can be used to go through the narrow channel.

The robot is in the landing state of the lower platform and changes the overall width of the mechanism by controlling the motors $M_1 - M_4$. Firstly, driving the motors M_5, M_8 at angular speed $\omega = \pi/2$ rad/s. When the driving angle is more than 43°, the robot realizes the first step of turning over. At this time, the two branches are on the ground. Continue to drive the motors M, M_8 at an angular speed of $\omega = 3\pi/4$ rad/s. Under the action of inertial force, the robot realized the second step of turning over. At this time, the upper platform landed. The simulation is shown in Fig. 20. Obviously, the minimum width of the robot can pass through the narrow channel and should be at the minimum position in the process of robot variable width, that is when $\theta_1 = \theta_3 = 45^\circ$, $\theta_2 = \theta_4 = -45^\circ$, which is $\sqrt{2}a$.

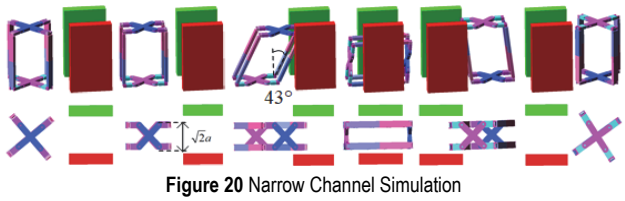

Figure 20 Narrow Channel Simulation

Because the omnidirectional rolling (including variable width) mode has a large contact surface with the ground and a large friction force, it is also suitable for climbing the slope. The slope climbing gait is simulated as show in Fig. 21.

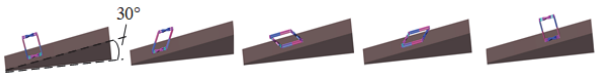

Figure 21 Robot climbing simulation

According to Fig. 21, when the robot is in the initial state of the climbing position, the robot's center of mass is closest to the edge of the support area (Fig. 22) and it is most likely to overturn. Therefore, this state is used as a constraint to calculate the maximum slope of the mechanism without turning over. Establish the CM motion mode and the relationship between G_{x_0} and slope angle is shown in Fig. 23.

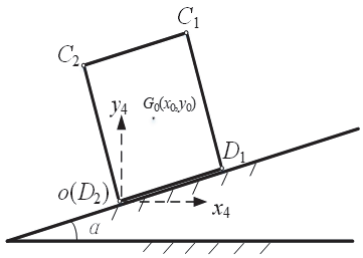

Figure 22 Variable width rolling climbing

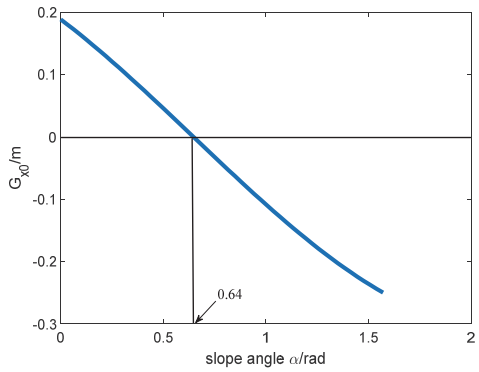

Figure 23 Robot omnidirectional (variable width) rolling mode climbing curve

It can be seen that the robot does not overturn when $G_{x_0} \geq 0$. That is, the maximum slope angle that the robot can climb stably in the omnidirectional (including variable width) rolling mode is 34°.

5.4 Simulation of Side Roll Mode Locomotion And Analysis Of Overreach Performance

The robot is in the state of double branches 1, 2 landing, and the steering of the four branches 1, 2, 3, 4 is controlled by driving the motors $M_1 - M_4$. When the steering angle controlled by the motor M_1 is greater than 78°, the robot's center of mass exceeds the support area. The robot tipped over and reached the state where the double-branched chains 1 and 4 landed, realizing a roll motion. The simulation is shown in Fig. 24.

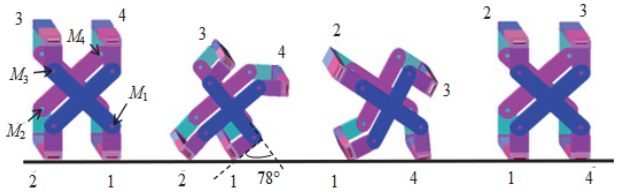

Figure 24 Rolling mode locomotion simulation

In the side rolling mode, the links 1, 2, 3 and 4 are in alternating contact with the ground, the contact area is small and the movement is dexterity, so it can be used to cross the steps and trenches. As shown, Fig. 25 is the simulation of robot crossing continuous step simulation; the height of the steps is 0.04 m and 0.08 m respectively.

Figure 25 Simulation across continuous steps

According to the climbing gait of the steps, when the robot falls over, the supporting links are changed from 1, 2 to 1, 4. In this process, the step platform is needed to provide enough support force and friction force to prevent the robot from sliding down. During the process of deformation and climbing, the CM needs to be moved from 1, 2 to 1, 4. From Fig. 32, it can be seen that the condition for the robot to successfully cross the obstacle is that the horizontal coordinates of the robot's CM coincide with the outer corner line of the step. When $G_{x_1} - L \geq 0$, the height of the step is the maximum height $H_{\max}$ the robot can cross the step.

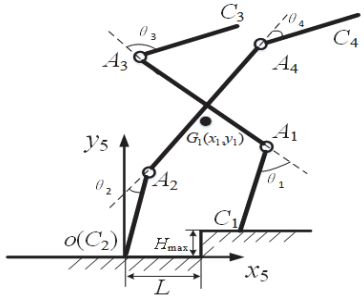

Figure 26 Analysis of the maximum step climbing height

Let step height mark as H, the distance between C_2 and step as L, set $\theta_3 = 3\pi/4$, $\theta_4 = \pi/4$ and A_1C_1 is parallel to A_2C_2. Fig. 33 shows the relationship between G_{x_1}, L and θ_1, H.

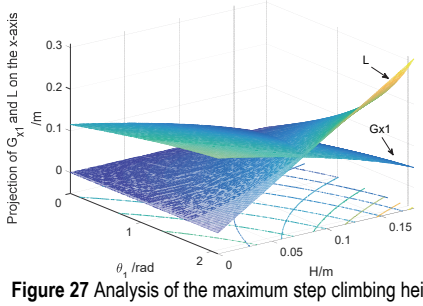

Figure 27 Analysis of the maximum step climbing height

From Fig. 27, it can be obtained that when $G_{x1} - L = 0$ and $\theta_1 = 7\pi/12$, the step height H is the maximum height that the robot can cross the step, which is 0.078 m.

Fig. 28 shows the simulation of the robot crossing the trench. The maximum width of the robot crossing a trench is $\sqrt{2}a$, which is 0.198 m.

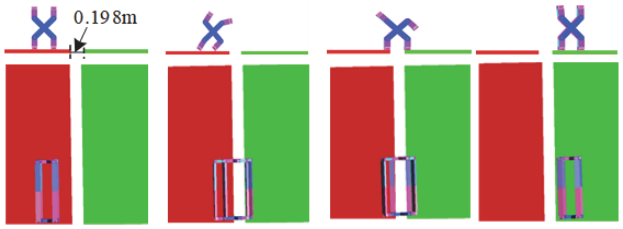

Figure 28 Crossing the trench simulation

5.5 Simulation Analysis of Spherical Rolling Mode

The robot is in the state where the single branch chain is on the ground, driving the motor on the ground branch chain to drive the robot to rotate. When the drive angle is more than 94°, the robot's center of mass exceeds the support area. After tilting and turning over, the next branch chain is on the ground. The robot moves forward as a whole as shown in Fig. 35.

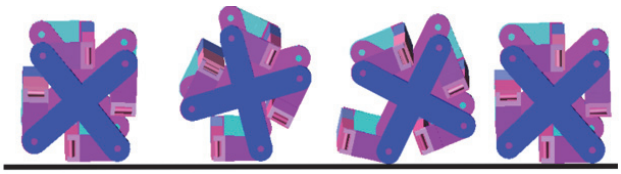

Figure 29 Spherical scroll mode

5.6 Simulation Analysis of Switching Between Four Locomotion Modes

The robot can adjust its attitude by changing eight input angles, and achieve four different locomotion modes. The switching of different locomotion modes can be realized through its corresponding transition state. Fig. 30 shows the simulation of robot switching from omnidirectional rolling mode to other modes. It can be seen that the mobile robot can switch to any other locomotion mode quickly and conveniently under the geometric deformation of the closed-loop of full R-joint mechanism. When the mobile robot encounters instability, it can use this characteristic to better return to the state of locomotion.

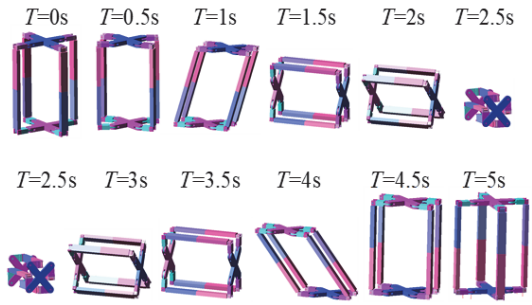

Figure 30 Simulation of each sport mode switching

6 PROTOTYPE AND EXPERIMENTS

A prototype of the mobile robot is designed and fabricated to verify the feasibility of the robot. Fig. 31 shows the prototype of the robot, and 8 motors are also marked in the figure.

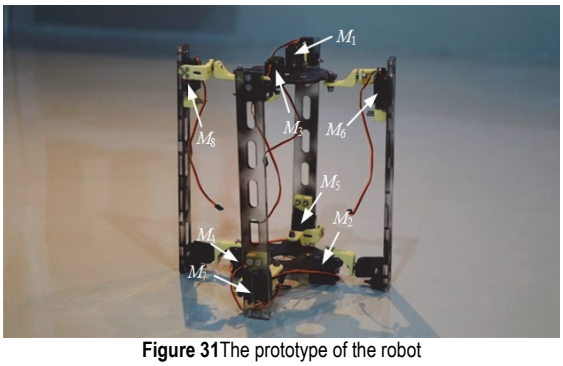

Figure 31 The prototype of the robot

Tab. 3 shows the details of the prototype. The total mass is 2.6 kg, the rod material is engineering plastics, and the joint material is aluminum alloy. In the initial state, the height of the mechanism is 500 mm and the width is 460 mm.

Table 3 the working states of motors

Parameter	Value
Mass / kg	2.6
Material	Aluminium alloy, engineering plastics
Motor model	MD996R
Working voltage	5

6.1 Omnidirectional Rolling Mode

Shown in Fig. 32 is one-cycle of omnidirectional rolling mode.

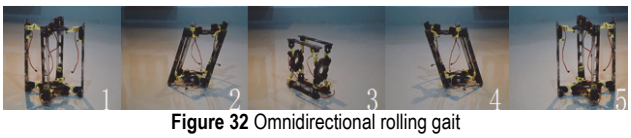

Figure 32 Omnidirectional rolling gait

6.2 Variable Width Rolling Mode

Fig. 33 shows the variable width rolling motion. In this mode, the robot can change the overall width of the mechanism by controlling the corresponding motors.

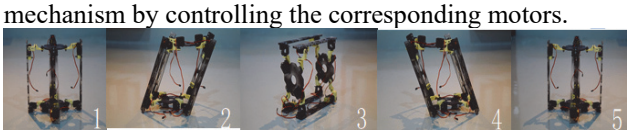

Figure 33 Variable width rolling gait

6.3 Side Rolling Mode

In the side rolling mode, the links are in alternating contact with the ground as shown in Fig. 34.

Figure 34 Side rolling gait

6.4 Spherical Rolling Mode

Fig. 35 shows the process of the spherical rolling motion. The robot moves forward as a whole.

Figure 35 Spherical rolling gait

7 C0NCLUSIONS

In order to improve the ground adaptability of mobile robots, an omnidirectional ground mobile robot based on single-loop full *R*-joint is proposed. The robot can realize four different rolling modes and switch from one to other by geometric deformation and mechanism reconstruction. The gait planning, locomotion feasibility analysis, and dynamics analysis have been carried out for the robot in different locomotion modes. The results have been verified by simulations and prototype experiments. The robot can adapt to different kinds of environment due to its deformation ability and multiple locomotion modes. It can be used to go through narrow channels, climbing steps, trenches, slopes and so on.

The multi-mode omnidirectional mobile robot consisting of two orthogonal closed-loops is also a symmetric 4-RRRRRR parallel mechanism. It has the advantages of high stiffness and precision of parallel mechanism in each rolling mode.

Compared with the existing robot, the robot's mechanism is simple, only composed of 14 connectors; the control system is simple, and four motion modes can be realized by time-sharing control of eight steering gears. It has the ability of omnidirectional rolling and self-recovery after overturning. The robot also has strong obstacle crossing ability, it can pass through 30°slope, can cross 0.04 m steps, and can pass through 0.198 m wide trenches. A narrow channel with a width of 0.198 m can be passed. In future work, the dynamic characteristics and control methods of the robot will be carried out.

8 REFERENCES

[1] Bai, L., Guan, J., Chen, X., Hou, J., & Duan, W. (2018). An optional passive/active transformable wheel-legged mobility concept for search and rescue robots. *Robotics and Autonomous Systems*, *107*, 145-155. https://doi.org/10.1016/j.robot.2018.06.005

[2] Cui, Y., Luo, Z., Shang, J., & Zhang, Z. (2018). Machine design of a reconfigurable wheel-track hybrid mobile robot with multi-locomotion. *Journal of Harbin Institute of Technology*, (7), 80-86.

[3] Lin, Y., Lin, H., & Lin, P. (2017). SLIP-Model-Based Dynamic Gait Generation in a Leg-Wheel Transformable Robot with Force Control. *IEEE Robotics and Automation Letters*, *2*(2), 804-810. https://doi.org/10.1109/ICRA.2015.7139921

[4] Arif, A. H., Waqas, M., Rahman, U. U., Anwar, S., Malik, A., & Iqbal, J. (2015). A hybrid humanoid-wheeled mobile robotic educational platform-design and prototyping. *Indian Journal of Science and Technology*, *7*(12), 2140-2148. https://doi.org/10.17485/ijst/2014/v7i12.24

[5] Pan, X., Xu, K., Wang, Y., & Ding, X. (2018). Design and analysis of a wheel-legged robot with a suspension system. *Robot*, *40*(3), 309-320.

[6] Niu, J., Wang, H., Jiang, Z., Chen, L., & Guo, S. (2020). Kinematic analysis of a serial-parallel hybrid mechanism and its application to a wheel-legged robot. *IEEE Access*, *8*, 111931-111944. https://doi.org/10.1109/ACCESS.2020.3001653

[7] Rachkov, M., Emelyanov, A., & Kolot, V. (2019). Reconfigurable Autonomous Wheel-Tracked Robot. *2019 International Conference on Industrial Engineering, Applications and Manufacturing (ICIEAM)*, Sochi, Russia. https://doi.org/10.1109/ICIEAM.2019.8742987

[8] Iqbal, J., Heikkila, S., & Halme, A. (2008). Tethertrackingand controlof ROSA robotic rover. *2008 10th International Conference on Control, Automation, Robotics and Vision*, Hanoi, Vietnam. https://doi.org/10.1109/ICARCV.2008.4795601

[9] Wang, Y., Tang, Z. & Dai, J. (2018). Kinematics and Gait Analysis of a Linkage-jointed Wheel-legged Robot. *Journal of Mechanical Engineering*, *54*(7), 11-19. https://doi.org/10.3901/JME.2018.07.011

[10] Luo, Z., Shang, J., Wei, G., & Ren, L. (2018). A reconfigurable hybrid wheel-track mobile robot based on watt ii six-bar linkage. *Mechanism & Machine Theory*, *128*, 16-32. https://doi.org/10.1016/j.mechmachtheory.2018.04.020

[11] Jiang, H., Xu, G., Zeng, W., & Gao, F. (2019). Design and kinematic modeling of a passively-actively transformable mobile robot. *Mechanism & Machine Theory*, *142*, 103591. https://doi.org/10.1016/j.mechmachtheory.2019.103591

[12] García, J. M., Martínez, J. L., Mandow, A., & García-Cerezo, A. (2017). Caster-leg aided maneuver for negotiating surface discontinuities with a wheeled skid-steer mobile robot. *Robotics & Autonomous Systems*, *91*, 25-37. https://doi.org/10.1016/j.robot.2016.12.007

[13] Wang, Z., Yao, Y., Zhang, D., Liu, Y., & Zhang, L. (2019). Redundantly actuated tetrahedron mobile robot structured by pure revolute joints. *Journal of Mechanical Engineering*, *55*(3), 18-26. https://doi.org/10.3901/JME.2019.03.018

[14] Liu, C., Yao, Y., Li, R., Tian, Y., Zhang, N., Ji, Y., & Kong, F. (2012). Rolling 4R linkages. *Mechanism & Machine Theory*, *48*, 1-14. https://doi.org/10.1016/j.mechmachtheory.2011.10.005

[15] Tian, Y., Zhang, D., Yao, Y., Kong, X., & Li, Y. (2017). A reconfigurable multi-mode mobile parallel robot. *Mechanism & Machine Theory*, *111*, 39-65. https://doi.org/10.1016/j.mechmachtheory.2017.01.003

[16] Liu, C., Chao, X., & Yao, Y. (2019). Multi-mode Spatial 6R Ground Mobile Mechanism. *Journal of Mechanical Engineering*, *55*(23), 38-47. https://doi.org/10.3901/JME.2019.23.038

[17] Wang, J., Yao, Y., & Kong, X. (2015). A rolling mechanism with two modes of planar and spherical linkages. *Proceedings of the Institution of Mechanical Engineers*, *Part C: Journal of Mechanical Engineering Science*, *230*(12), 2110-2123 https://doi.org/10.1177/0954406215590188

[18] Tian, Y., Wei, X., Joneja, A., & Yao, Y. (2014). Sliding-crawling parallelogram mechanism. *Mechanism & Machine Theory*, *78*, 201-228. https://doi.org/10.1016/j.mechmachtheory.2014.03.013

[19] Tian, Y., Yao, Y., & Wang, J. (2014). A rolling 8-bar linkage mechanism. *Journal of Mechanisms & Robotics. 7*(4) 041002. https://doi.org/10.1115/1.4029117

[20] He, Y., Li, R., Wu, J., Liu, X., & Yao, Y. (2019). Design and Mobility Analysis of a Multi-Mode Two-Wheel Mobile Robot. *Journal of Mechanical Engineering*, *55*(23).

[21] Liu, C., Li, R., & Yao, Y. (2012). An omnidirectional rolling 8u parallel mechanism. *Journal of Mechanisms & Robotics*, *4*(3), 1058-1058. https://doi.org/10.1115/1.4006657

[22] Wang, J., Yao, Y., & Kong, X. (2018). A reconfigurable tri-prism mobile robot with eight modes. *Robotica*, *36*(10), 1454-1476. https://doi.org/10.1017/S0263574718000498
[23] Zhang, C., Wan, Y., Zhang, D., & Ma, Q. (2019). A New Mathematical Method to Study the Singularity of 3-RSR Multimode Mobile Parallel Mechanism. *Mathematical Problems in Engineering*, 1563-5147. https://doi.org/10.1155/2019/1327167
[24] Phipps, C., Shores, B., & Minor, M. (2008). Design and quasi-static locomotion analysis of the rolling disk biped hybrid robot. *IEEE Transactions on Robotics*, *24*(6), 1302-1314. https://doi.org/10.1109/TRO.2008.2007936
[25] Li, Y., Yao, Y., & He, Y. (2018). Design and analysis of a multi-mode mobile robot based on a parallel mechanism with branch variation. *Mechanism and Machine Theory*, *130*, 276-300. https://doi.org/10.1016/j.mechmachtheory.2018.07.018
[26] Huang, Z., Zhao, Y., & Zhao, T. (2014). *Advanced Spatical Mechanism*. Beijing, BJ: Higher Education Press.
[27] Liu, X., Zhang, C., Ni, C., & Lu, C. (2019). A reconfigurable multi-mode walking-rolling robot based on motor time-sharing control. *Industrial Robot: The International Journal of Robotics Research and Application*, *47*(2), 293-311. https://doi.org/10.1108/IR-05-2019-0106

Contact information:

Chunyan ZHANG, Associate professor
(Corresponding author)
1) Institution College of Mechanical Engineering, Donghua University,
No. 2999, North Renmin Road, Songjiang District,
Shanghai, P.R. China. 201620
2) School of Mechanical and Automotive Engineering, Shanghai University of Engineering Science,
No.333, Longteng Road, Songjiang District,
Shanghai, P.R. China 201620
E-mail: keke204102@163.com

Xinxing JIANG, Master
School of Mechanical and Automotive Engineering, Shanghai University of Engineering Science,
No.333, Longteng Road, Songjiang District,
Shanghai, P.R. China. 201620
E-mail 1752436046@qq.com

Xiangyu LIU, Master
Institution College of Mechanical Engineering, Donghua University,
No. 2999, North Renmin Road, Songjiang District,
Shanghai, P.R. China. 201620
E-mail: 1364459057@qq.com

Dan ZHANG, Professor
Institution College of Mechanical Engineering, Donghua University,
No. 2999, North Renmin Road, Songjiang District,
Shanghai, P.R. China. 201620
Email: dzhang99@yorku

Table of variables in this paper

Symbol	Meaning	Unit
X、Y、Z	Coordinate axis	
A、F	Each endpoint of upper and lower platform	
B、C	The end of each connector	
D、E	The end points of four branched chains	
2a	Length of upper and lower platform	m
b	Length of connector AICI	m
l	Length of limb	m
R	Rotating pair	
θ_1、θ_3	Rotation angle of limb 1 and 3 around rotation pair $R_{11}R_{16}$ and $R_{31}R_{36}$	rad
θ_5、θ_7	Rotation angle of limb1 and 3 around rotation pair R_{14} and R_{34}	rad
θ_6、θ_8	The limb 2 and 4 constitute the rotation angle around the rotation pair R_{24} and R_{44}	rad
θ_2、θ_4	Rotation angle of limb 2 and 4 around rotation pair $R_{21}R_{26}$ and $R_{41}R_{46}$	rad
M	Motor	
g	Acceleration of gravity	M/s^2
J	Moment of inertia	$Kg.m^2$
α	Angular acceleration	rad/s
m	Bar mass	kg
G	Centroid	
ω	Angular velocity of motor	rad/s
H	Step height	m
L	C_2 distance to step	m

Table of current robot development

Type of robot	typical example	Strengths/Disadvantages
Traditional omnidirectional mobile robot		It has three kinds of gait, but the structure is complex.
	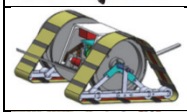	It can switch between wheeled and crawler motion, and cannot pass through narrow channels and other terrain.
		It can pass through the terrain such as steps and slopes, but it is huge and complex to control.
Multi mode robot based on link configuration	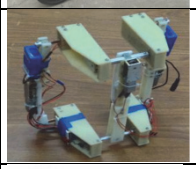	It has more movement modes, but it is easy to lose movement ability after overturning.
		It can pass through steps, slopes and other terrain, but the movement mode is less.
	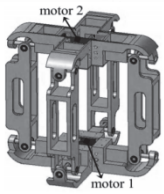	The mechanism is simple, but the movement mode is single.
	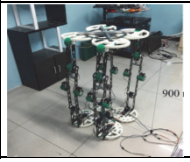	It has more movement modes, but it is easy to lose movement ability after overturning.